GPS Civil Signal Self-Interference Mitigation During Weak Signal Acquisition

Yu T. Morton, Mikel Miller, James Tsui, David Lin, and Qihou Zhou

***Abstract*—Current global positioning system receivers can acquire weak satellite signals with $C/N_0 = 15$ dB/Hz if there is no self-interference from other strong satellite signals. This correspondence presents a computational efficient partitioned subspace projection method to mitigate the self-interference. The method is evaluated using simulated signals and a block-based weak signal acquisition algorithm.**

***Index Terms*—Global positioning system (GPS) receiver, partitioned subspace projection, self-interference mitigation, weak signal acquisition.**

I. Introduction

The global positioning system (GPS) is a direct-sequence spread-spectrum (DS-SS) code-division multiple access (CDMA) system. The L1 band GPS civil signals use 1023-chip pseudorandom (PRN) sequences (C/A code) with a chip rate of 1.023 MHz to modulate the 1.57542 GHz carrier. A GPS receiver acquires and tracks a satellite signal by correlating the receiver input signal with a locally generated carrier and a replicate C/A code sequence. Maximum correlation occurs when the local carrier Doppler frequency and the replicate C/A code phase match those of a satellite signal contained in the input. During the acquisition of a weak signal, cross-correlation of the weak signal with other strong signals in the input gives rise to two problems. First, the cross-correlation between the strong and the weak signals may be compatible with or surpass the weak signal autocorrelation peak. Second, the cross-correlations between strong signals and a weak signal's local replicate contribute to the pre-detection noise floor, effectively reducing the weak signal acquisition processing gain. [10] showed that the self-interference can lead up to 9 dB processing gain degradation in the weak signal acquisition.

The mitigation of self-interference on GPS signal acquisition was dealt with in [4]–[6], [9], [14]. In [9], the self-interference problem is encountered in a GPS system augmented by ground-based pseudolites. A successive interference cancellation (SIC) technique is used to mitigate the pseudolites' interferences. To acquire a very weak GPS signal in the presence of other stronger GPS signals is more challenging because it involves extended coherent and non-coherent integration of the incoming signals [1], [7], [11], [15]. The Doppler frequency and oscillator effects may cause a noticeable interfering signal carrier and code phase shift during the extended integration time, making it difficult to maintain an accurate reconstruction of the interfering satellite signals.

Manuscript received March 5, 2007; revised April 18, 2007. The associate editor coordinating the review of this manuscript and approving it for publication was Dr. Erchin Serpedin.This work was supported in part by the Air Force Office of Scientific Research (AFOSR) and the Air Force Research Laboratory (AFRL) under Contract F49620-03-1-0225.

Y. T. Morton and Q. Zhou are with the Department of Electrical and Computer Engineering, Miami University, Oxford, OH 45056 USA (e-mail: mortonyt@muohio.edu; zhouq@muohio.edu).

M. Miller is with the Air Force Research Laboratory, Eglin Air Force Base, FL 32542-6810 USA (e-mail: mikel.miller@eglin.af.mil).

J. Tsui and D. Lin are with the Air Force Research Laboratory, Wright Patterson Air Force Base, OH 45433 USA (e-mail: James.Tsui@wpafb.af.mil; david.lin@wpafb.af.mil).

Color versions of one or more of the figures in this correspondence are available online at http://ieeexplore.ieee.org.

Digital Object Identifier 10.1109/TSP.2007.900761

References [4] and [5] presented an innovative approach that utilized modified despreading codes that were different from the weak signal PRN code under acquisition. The modified despreading code was selected to be orthogonal to the PRN codes of the strong signals in the input. The method is attractive for lower-end GPS receivers with 1 to 2 bits ADCs because even strong GPS signals are well below the receiver noise level. The SIC type approach will not be effective in eliminating strong signals from the input. There are two drawbacks of the method. First, because the relative Doppler frequencies of the interfering signals continuously change, the despreading codes also have to be adjusted accordingly. Secondly, it is difficult to find a despreading code that is orthogonal to multiple strong satellite signals in the input.

The delayed parallel interference cancellation (DPIC) method proposed by [6] handles the self-interference at the post-correlation stage. The method estimates post-correlation cross correlation for each strong signal, then subtracts the cross correlations from the input correlation outputs. The method overcomes the ineffectiveness of strong signal cancellation in receivers with low bit numbers. The disadvantage of the method is that it requires additional correlators for each strong-weak signal pair.

The subspace projection method is a technique that has found applications in rejecting interferences involving signals that are not orthogonal to each other [2], [3]. A number of problems for detecting signals in subspace interference and broadband noise were formulated in [13]. Several implementation approaches for applying the subspace projection method to mitigate GPS self-interference were suggested in [14]. Most of these methods require excessive computing power for implementation of weak GPS signal acquisition. This correspondence presents a computationally efficient approach that performs interference subspace projection on partitioned input data blocks. A batch-based weak GPS signal acquisition algorithm is used to evaluate the effectiveness of this partitioned subspace interference cancellation approach. This correspondence discusses the interference subspace projection algorithm, presents simulation and analysis of the interference cancellation residual errors, and evaluates the resulting weak signal acquisition performance.

II. Self-Interference Cancellation Using Subspace Projection Method

Vector-valued linear signal representation can be applied to a GPS receiver's digital input

$$\begin{aligned} \vec{s} &= \overleftarrow{S}\,\vec{a}_s, \\ \vec{w} &= \overleftarrow{H}\,\vec{a}_w, \\ \vec{y} &= \vec{s} + \vec{w} + \vec{v}. \end{aligned} \tag{1}$$

Here, $\vec{y} \in C^{n\times 1}$ contains the down-converted receiver baseband data samples. $\vec{s} \in C^{n\times 1}$ and $\vec{w} \in C^{n\times 1}$ contain the strong and weak signals, respectively. $\overleftrightarrow{S} \in C^{n\times m}$ is a $n \times m$ matrix whose m columns represent m strong signal vectors with unit amplitude. $\overleftrightarrow{H} \in C^{n\times k}$ is a $n \times k$ matrix whose k columns represent k weak signal vectors with unit amplitude. $\vec{a}_s \in C^{m\times 1}$ and $\vec{a}_w \in C^{k\times 1}$ contain the amplitudes of the strong and weak signal amplitudes, respectively. $\vec{v} \in C^{n\times 1}$ is the receiver noise vector.

The strong signal subspace spanned by the columns of the matrix $\vec{S}$ (denoted as $\langle \mathbf{S} \rangle$) and the weak signal subspace spanned by the columns of matrix $\overleftarrow{H}$ (denoted as $\langle \mathbf{H} \rangle$) are near orthogonal to each other. Using notations developed in [3], Fig. 1 illustrates the relationship among the input signal vector and its orthogonal and oblique projections onto its member subspaces. P_S, P_H, and P_{SH} are the orthogonal projection operators for projection onto the $\langle \mathbf{S} \rangle$, $\langle \mathbf{H} \rangle$, and the joint $\langle \mathbf{SH} \rangle$ subspaces,

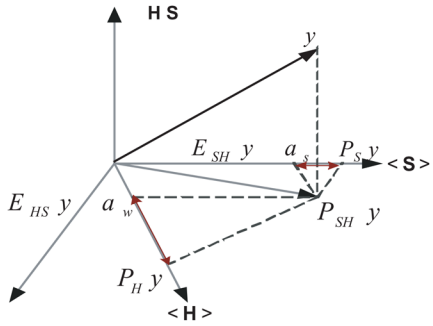

Fig. 1. Illustrative view of input signal vector, its subspace components, and orthogonal and oblique projections of the signal vector onto its subspaces.

respectively. The true vector weights of the strong and weak signals are the oblique projections (E_{HS} and E_{SH}) of the input signal vector onto the strong and weak signal subspaces. The oblique projection operator based detection test statistic of the subspace signal in structured subspace interference and noise was formulized by [2] and [13]. Reference [14] applied the oblique projection operator E_{HS} and the test statistics described by [13] to replace the standard correlation process in GPS signals acquisition. This test statistic, however, is computationally expensive. This is particularly true for weak signal processing, where an extended input data length and hence very large matrix and vector sizes are involved.

On the other hand, the orthogonal projection of the total input $\vec{y}$ onto the strong signal subspace $\langle \mathbf{S} \rangle$, $P_S \vec{y}$, is a good approximation of the true strong signal contribution to the total input signal

$$\begin{aligned} P_S \vec{y} &= \overleftrightarrow{S}(\overleftrightarrow{S}^T \overleftrightarrow{S})^{-1} \overleftrightarrow{S}^T \vec{y} \\ &= \overleftrightarrow{S}(\overleftrightarrow{S}^T \overleftrightarrow{S})^{-1} \overleftrightarrow{S}^T (\overleftrightarrow{S}\vec{a}_s + \overleftrightarrow{H}\vec{a}_w + \vec{v}) \approx \overleftrightarrow{S}\vec{a}_s + \vec{v}'. \end{aligned} \quad (2)$$

The term $[\overleftrightarrow{S}(\overleftrightarrow{S}^T \overleftrightarrow{S})^{-1}(\vec{S}^T \overleftrightarrow{H})]\vec{a}_w$ is the negligible cross-correlation interference of the weak signals on the strong signals because it is ~ 23.9 dB below the strong signal auto-correlation peak, and $|\vec{a}_W| \ll |\vec{a}_S|$. The term $\vec{v}'$ is the random noise projected onto the strong signal subspace.

Equation (2) indicates that the projection of the input $\vec{y}$ onto the strong signal subspace $\langle \mathbf{S} \rangle$ is the sum of the strong satellite signals and noise projection $\langle \mathbf{S} \rangle$. If we use $P_S \vec{y}$ as an estimate of the strong signals, there are two main error terms: (1) $\Delta\vec{v} = \vec{v} - \vec{v}'$, and (2) $\Delta\vec{\varepsilon}$ due to deviation of the tracked strong signal parameters (Doppler frequency, carrier, and code phase) from their true values

$$\Delta\vec{y} = \vec{y} - P_s\vec{y} \approx \overleftrightarrow{H}\vec{a}_w + \Delta\vec{v} + \Delta\overleftrightarrow{\epsilon}. \quad (3)$$

If $\Delta\vec{y}$ is comparable with or below the receiver noise, the weak signal acquisition procedure can be applied to $\Delta\vec{y}$ with negligible impact from the strong signal interference.

III. Partitioned Subspace Projection Residual Error

To evaluate the projection error $\Delta\vec{\varepsilon}$, we simulated an input signal consisting of a strong and a weak GPS signal and random noise. We constructed the strong signal subspace using the signal's true code phase, while allowing error in its Doppler frequency. We computed the difference between the true strong signal and the projection as a function of the Doppler frequency error Δf. The projection was performed over a 200-ms data interval to characterize the error associated with the typical data length used in the weak signal acquisition process. Such an extended data length presents a significant amount of error in the projection due to even a very small Doppler frequency deviation. For example, if a strong signal Doppler frequency has a tracking error of $\Delta f = 1.5$ Hz, it will translate into a carrier phase offset $\Delta\phi = 2\pi\Delta f \times 200 \text{ ms} = 0.6\pi$ over 200 ms. Projection of the input onto a subspace with this type of misalignment will generate unacceptable projection errors. Fig. 2(a) compares a GPS signal (solid line) with its projection counterpart (dashed line) using $\Delta f = 3$ Hz. The signals are sampled at 5 MHz. The initial carrier and code phase of the subspace is aligned with the true signal. The upper panel in Fig. 2(a) contrasts the first and last 50 samples of the original and the projected signal in 200-ms data. Notice the obvious difference in the last 50 samples. The lower panel plots the entire 200-ms data block and its projection. Note that the differences between the original and projected data grow as the time increases.

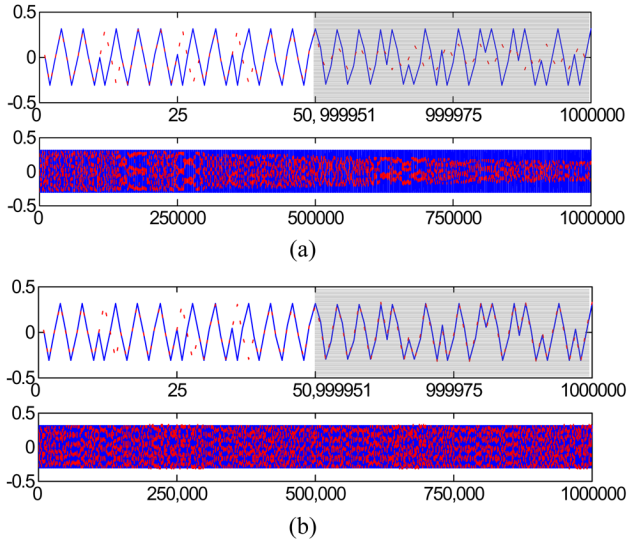

Fig. 2. Comparison of a GPS signal (solid line) and its subspace projected version (dashed line). The subspace signal contains a 3 Hz Doppler frequency error. (a) Projection is performed for an entire 200-ms data. (b) Partitioned projection is performed for each 10-ms blocks. The top panels contain the first and the last 50 samples while the lower panels contain the entire sequence of data samples.

In the partitioned projection approach, we divide the input data block into L smaller subblocks of length T, as shown in Fig. 3. Within a subblock $i (i = 1, 2, \ldots L)$, a signal subspace is constructed using the code phase $\hat{n}_i$, Doppler frequency $\hat{f}_{di}$, and initial carrier phase $\hat{\phi}_i$, generated from the batch-based strong signal tracking algorithms for each subblock. Each subblock input signal is projected onto its corresponding subspace.

Using the same data set in Fig. 2(a), we plotted the partitioned subspace projection results in Fig. 2(b). We chose a partition size of 10 ms. Note the relatively small differences between the original and the projected signal throughout the entire 200-ms data sequence. To obtain a more quantitative measure of the interference residual error using the partitioned subspace projection procedure, we simulated strong signals with signal to noise ratio $\text{SNR} = -13$ and -19 dB (corresponding to $C/N_0 = 50$ and 44 dB/Hz, respectively) and computed their interference residual error. We allowed Δf to vary from 0 to 100 Hz. For each Δf value, we performed 50 simulations with randomly varying signal carrier and code phase within their realistic range limits. To simplify the comparisons, we generated the signals using normalized noise power. Fig. 4 plots the simulation results. For $|\Delta f| \leq \pm 5$ Hz, the interference residual error power is less than -30 dBW which is far below the original input interfering signal power of -13 and -19 dBW. This residual error power level is no longer a threat to weak signal (of power level

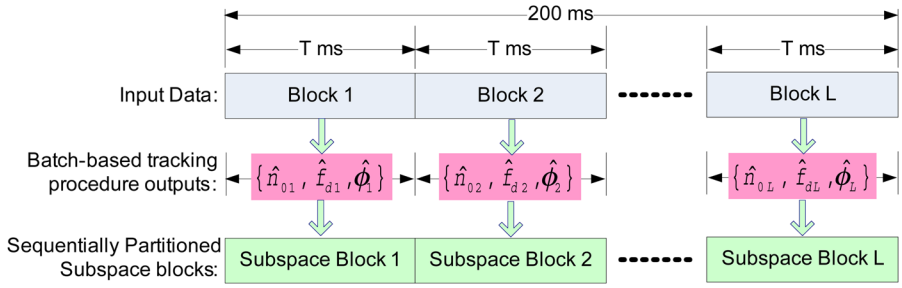

Fig. 3. Partition of projection subspace into sequential subblocks for reduced projection error.

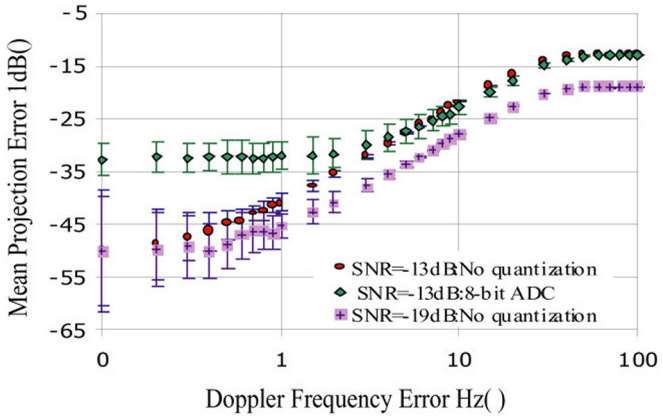

Fig. 4. Simulated projection error as a function of Doppler frequency error.

between -40 to -36 dBW) acquisition. As the Δf increases to about 50 Hz, the interference residual error power reaches the corresponding input interfering signal power level. The partitioned subspace projection method loses its effectiveness. In a steady-state tracking mode, however, Δf is typically within a few Hz which guarantees that the projection method will have negligible interference residual power to impact the weak signal acquisition.

We also simulated inputs that are quantized using an 8-bit ADC sampled at 5 MHz frequency. The result for strong signal $\mathrm{SNR} = -13$ dBW is shown in Fig. 4 as a comparison. For this type of high-end receiver, the quantization raised the projection error levels considerably for $|\Delta f| \leq \pm 5$ Hz. But the amount of the project error is still about 20 dB below the original strong signal power. For low-end receivers with only 1–2 bit ADCs, the interference residual error will be too large for the method to be effective.

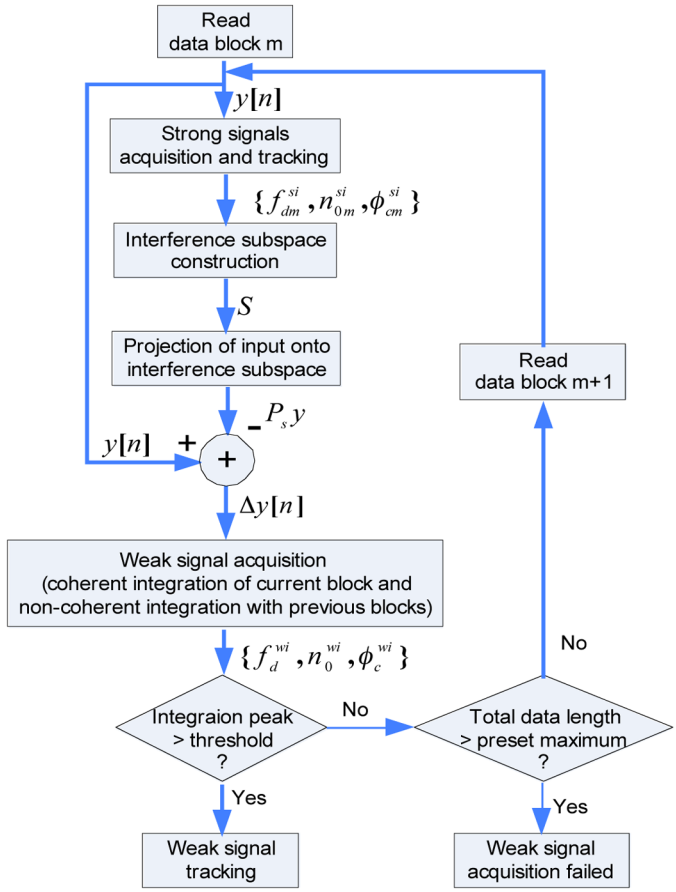

Fig. 5. Self-interference removal and weak signal acquisition algorithm.

IV. Interference Cancellation Algorithm Performance Evaluation

To evaluate the effectiveness of the partitioned projection method in canceling strong signal interference, we applied the algorithm as depicted in Fig. 5 to simulated GPS signals. The figure shows the block diagram for one data block processing. The strong satellite signal parameters (Doppler frequency f_{dm}^{si}, code phase n_{0m}^{si}, carrier phase ϕ_{cm}^{si}, and navigation data on the strong signals) are obtained from the batchbased software tracking routines. These parameters are used to construct the interference subspace $\boldsymbol{S}$. Projection of the input signal onto this subspace, $\boldsymbol{P}_s y$, provides an estimate of the interference signal. The difference between the input and the projection $\Delta y[n]$ contains negligible weak signal contributions, noise, and projection error $\Delta\varepsilon[n]$. Coherent integration of $\Delta y[n]$ within this block of data is performed. The result is then non-coherently integrated with the output of coherent integrations of previous data blocks. The resulting peak integration value is compared with a predetermined threshold to determine if weak signal acquisition has been successful. Successfully acquired weak signals will be further processed through tracking loops. If the integration peak is below the threshold, the next data block will be read and the above processing will be repeated. This process is repeated until the weak signal is acquired, or when the total data length exceeds a preset maximum value.

We implemented the weak signal acquisition algorithm described in [15]. This method applies the FFT-based coherent integration procedure to consecutive 10-ms input data blocks, generating 100 Hz output frequency bins. If the receiver front end bandwidth is 2 MHz, this coherent integration will lead to a processing gain of 43 dB. The presence of a weak signal navigation data bit within a data block will degrade the coherent integration gain of that block. The processing gain associated

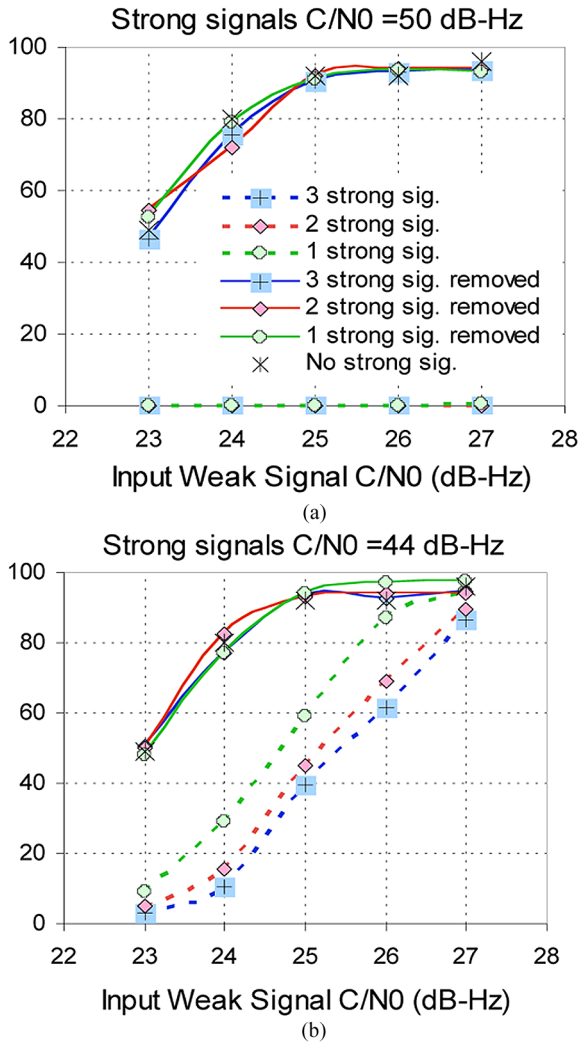

Fig. 6. Acquisition success rate as a function of the weak signal input C/N_0 before (dashed line) and after (solid line) application of interference cancellation for inputs having 0, 1, 2, and 3 strong signals in the inputs. The strong signal C/N_0 is (a) 50 dB/Hz and (b) 44 dB/Hz.

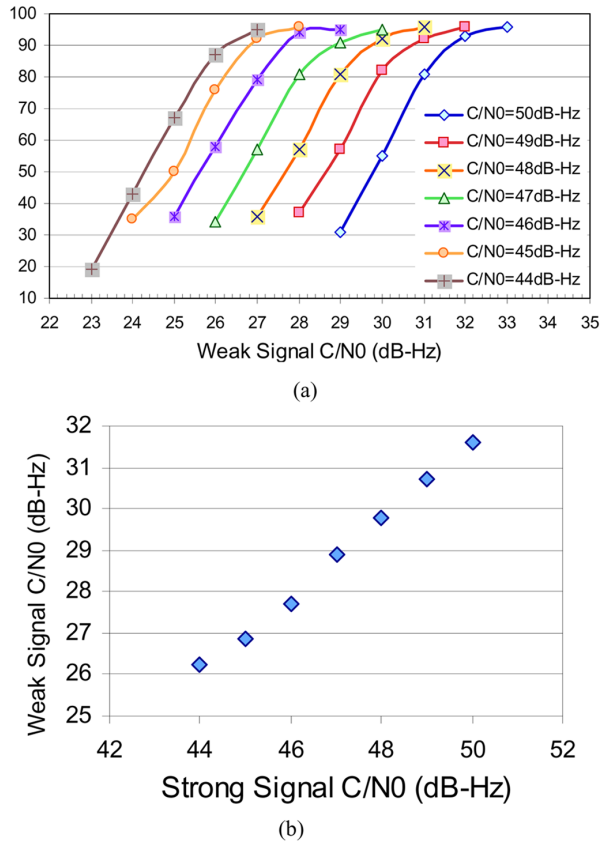

Fig. 7. Weak signal acquisition performance without strong signal interference mitigation: (a) Weak signal acquisition success rate as a function of input C/N_0 in the presence of three strong interfering signals whose C/N_0 is indicated in the legend. (b) The minimum weak signal's input C/N_0 to achieve 90% successful acquisition rate as a function of co-existing strong signal C/N_0.

with the non-coherent integration has been documented in [15]. There are several methods that allow block-based software acquisition algorithms to overcome the impact of the navigation data bit on acquisition [1], [12]. Therefore, we omit the weak signal navigation data issue here to focus on the performance of interference cancellation.

We performed weak signal acquisition using 200-ms data partitioned into 10-ms blocks, sampled by an 8-bit ADC at 5 MHz. Fig. 6 plots the acquisition success rate as a function of the weak signal C/N_0. The solid curves are obtained from input that originally contained 1, 2, and 3 strong signals, respectively. All strong signals' C/N_0 are 50 dB/Hz in Fig. 6(a) and 44 dB/Hz in Fig. 6(b). For comparison, the dashed lines are the acquisition results of applying acquisition algorithms directly to the input data prior to interference cancellation. The symbol "$*$" indicates the weak signal acquisition algorithm performance when there is no strong signal in the input. The input signal's Doppler frequencies and code and carrier phases are assigned uniformly distributed random values within their allowed ranges. Each data point is the result of 500 simulation runs. Note that the acquisition success rate obtained having one, two, and three strong signals after interference removal is comparable to the results when no strong signal is present. Without interference cancellation, the weak signal detection rate is nearly 0 across the board for strong signal with $C/N_0 = 50$ dB/Hz. For strong signals with $C/N_0 = 44$ dB/Hz, the weak signal acquisition performance improves as the weak signal C/N_0 approaches 27 dB/Hz, despite the presence of the strong signals. Also note that the number of strong signals in the input data does not affect the interference cancellation performance.

We further performed simulations to acquire weak signals without interference cancellation for a wider range of input signal levels. Fig. 7(a) showed the weak signal acquisition success rate for input containing one strong satellite. The strong and weak signal C/N_0 ranges 44∼50 dB/Hz and 23∼33 dB/Hz, respectively. Each data point is obtained from 500 simulation runs. From this figure we can estimate the input weak signal C/N_0 at which its acquisition success rate reaches 90%. Fig. 7(b) plots this weak signal C/N_0 as a function of the strong signal C/N_0. This figure shows that without interference cancellation, there is an almost linear relationship between the strong signal power and the minimum input weak signal power that meets the 90% detection rate. For a strong signal with $C/N_0 = 50$ dB/Hz and 44 dB/Hz, the minimum weak signal power levels at which we can guarantee 90% detection rate are 31.6 dB/Hz and 26.2 dB/Hz, respectively. We also performed simulations for the cases where two and three signals co-exist with the weak signals. The results are nearly identical to the one strong signal case.

Our earlier simulation results, as shown Fig. 6, indicate that when there is no strong signal in the input, this algorithm requires the weak signal $C/N_0 = 25$ dB/Hz in order to achieve a 90% detection rate. Compared to the results shown in Fig. 7(b), we conclude that the presence of a signal with $C/N_0 = 44$ dB/Hz raises the detectable weak

signal level by about 1.2 dB. For each additional 1 dB increase in the strong signal power level, the weak signal level having a 90% detection rate increases by ∼0.93 dB.

The partitioned projection method is computationally feasible to implement. This is evident from observing (2): $\overleftarrow{S} \in C^{n \times m}$ and $\vec{y} \in C^{n \times 1}$ where m is the number of strong signals in the input and n is the number of input data samples in one partition. Assuming $m = 3$ and $n = 50\ 000$ (10-ms data block sampled at 5 MHz), (3) involves 7.5×10^5 multiplications. Considering that the weak signal acquisition operation on the same 10-ms data using frequency domain coherent integration method requires $\sim 1.05 \times 10^6$ multiplications [15, pp. 139], this computational cost is quite reasonable.

The partitioned subspace projection method is a robust and efficient method compared to the methods described in [4]–[6]. References [4] and [5] use modified despreading codes that were different from the weak signal PRN code under acquisition and the method breaks down in the presence of four or more strong signals. The post-correlation cross-correlation mitigation method presented in [6] was shown to be able to detect weak signals co-existing with up to four strong signals that were each 23 dB stronger, although there is no statistical performance data presented in [6]. And this method requires a large number of correlators in implementation. As shown in Fig. 6(a), the partitioned subspace projection method achieves 90% weak signal detection rate with three 23 dB+ strong signals. Our additional simulations involving up to six strong signals in the input show that the partitioned subspace projection method performance is not much affected by the number of strong signals. The one disadvantage associated with the partitioned subspace projection method is the requirement on the ADC resolution. The simulation results presented in this correspondence are all based on an 8-bit ADC. The method is not effective if only 1- or 2-bit ADCs are used in the front end.

V. Conclusion

This correspondence presents a partitioned subspace projection method to mitigate the cross-correlation interference on weak GPS signal acquisition. The partitioned projection method divides the input data into subblocks. Batch-based strong signal tracking loop outputs are used to construct the interference subspace for each subblock. Subspace projection and interference cancellation are performed for each individual subblock. Weak signal acquisition is performed coherently over each subblock. The outputs of the coherent integrations are non-coherently integrated to further improve the weak signal acquisition processing gain. Our simulations show that the partitioned subspace projection represents a good approximation of the interference contribution to the total input. We successfully applied weak signal acquisition to the difference between the input and the projection. Simulations demonstrated the effectiveness of this interference cancellation method for input that contains one, two, and three strong signals in the possible strong signal power range.

Our simulation also demonstrated the impact of self-interference on the outcome of the weak signal acquisition procedure. We showed that the presence of a GPS signal with $C/N_0 = 44$ dB/Hz raises the minimum detectable weak signal level by approximately 0.93 dB for every 1 dB increase in the strong signal power level. The number of strong signals does not appear to affect the results.

References

[1] D. M. Akos, P. Normark, J. Lee, K. G. Gromov, J. B. Tsui, and J. J. Schamus, "Low power global navigation satellite systems (GNSS) signal detection and processing," in *Proc. ION GPS-2000*, Salt Lake City, UT, Sep. 2000, pp. 784–791.

[2] R. T. Behrens and L. L. Scharf, "Signal processing applications of oblique projection operators," *IEEE Trans. Signal Process.*, vol. 42, no. 6, pp. 1413–1423, Jun. 1994.

[3] B. Friedlander, "A signal subspace method for adaptive interference cancellation," *IEEE Trans. Acoust., Speech, Signal Process.*, vol. 36, no. 8, pp. 1835–1845, Aug. 1988.

[4] E. P. Glennon and A. G. Dempster, "A novel cross correlation mitigation technique," presented at the ION GNSS, Long Beach, CA, Sep. 2005.

[5] E. P. Glennon and A. G. Dempster, "Cross correlation mitigation by adaptive orthogonalization using constraints—New results," presented at the ION GNSS, Fort Worth, TX, Sep. 2006.

[6] E. P. Glennon, R. C. Bryant, and A. G. Dempster, "Delayed parallel interference cancellation for GPS C/A code receivers," in *Proc. IAIN/GNSS*, Jeju, Korea, Oct. 2006, pp. 261–266.

[7] D. M. Lin, J. B. Tsui, L. L. Liou, and Y. T. Morton, "Sensitivity limit of a stand-alone GPS receiver," in *Proc. ION GPS*, Portland, OR, Sep. 2002, pp. 1663–1667.

[8] S. Kayalar and H. L. Weinert, "Oblique projections: Formulas, algorithms, and error bounds," *Math. Contr. Signals Syst.*, vol. 2, no. 1, pp. 33–45, 1989.

[9] P. H. Madhani, P. Axelrad, K. Krumvieda, and J. Thomas, "Application of successive interference cancellation to the GPS pseudolite near-far problem," *IEEE Trans. Aerosp. Electon. Syst.*, vol. 39, no. 2, pp. 481–488, Apr. 2003.

[10] Y. T. Morton, J. B. Tsui, D. M. Lin, M. M. Miller, J. Schamus, Q. Zhou, and M. P. French, "Assessment and handling of C/A code self-interference during weak GPS signal acquisition," in *Proc. ION GPS*, Portland, OR, Sep. 2003, pp. 646–653.

[11] M. L. Psiaki, "Block acquisition of weak GPS signals in a software receiver," in *Proc. ION GPS*, Salt Lake City, UT, Sep. 2001, pp. 2838–2850.

[12] A. Soloviev, S. Gunawardena, and F. van Graas, "Deeply integrated GPS/low-cost IMU for low CNR signal processing: Flight test results and real time implementation," presented at the ION GNSS, Long Beach, CA, Sep. 2004.

[13] L. L. Scharf and B. Friedlander, "Matched subspace detectors," *IEEE Trans. Signal Process.*, vol. 42, no. 8, pp. 2146–2157, Aug. 1994.

[14] J. Thomas, W. Kober, E. Olson, and K. Krumvieda, "Interference cancellation in a signal," U.S. Patent 6 711 219 B2, 2004.

[15] J. B. Tsui, *Fundamentals of Global Positioning System Receivers, a Software Approach*, 2nd ed. New York: Wiley, 2004, pp. 224–270.